ChemComm

COMMUNICATION

Published on 11 May 2026

Cite this: *Chem. Commun.*, 2026, **62**, 10950

Received 6th March 2026,
Accepted 10th May 2026

DOI: 10.1039/d6cc01370h

rsc.li/chemcomm

Diarylethene-powered photo-switching between precipitated nanostrips and dispersed supramolecular polymers

Katsuyuki Murai,[a] Honami Matsui,[b] Tatsuya Seki,[a] Takayuki Umakoshi,[b] Christian Ganser,[c] Takashi Kajitani,[d] Sougata Datta,[e] Hiroki Hanayama[f] and Shiki Yagai *[ef]

UV and visible light irradiation reversibly switches diarylethene-based supramolecular assemblies between precipitated, ordered nanostrip aggregates and uniformly dispersed supramolecular fibers in a nonpolar solvent by modulating conformational freedom.

Controlling the aggregation behavior of supramolecular polymers (SPs) is essential for translating molecular design into practical materials. Molecular design must address not only the primary one-dimensional architecture of supramolecular polymers but also their propensity for higher-order organization, *i.e.*, bundling or lateral association, which ultimately governs solubility, processability, and bulk material properties.[1–8] In this context, supramolecular polymer polymorphism offers powerful opportunities: a single monomer can access multiple one-dimensional morphologies and their distinct higher-order aggregation states.[9–14] Yet, reversible interconversion between such one-dimensional morphologies remains challenging because each assembled state is typically stabilized by a different balance of noncovalent interactions and entropic penalties and is frequently kinetically separated by substantial barriers.

In this regard, photochromic molecules offer an attractive strategy to regulate the structural organization of supramolecular polymers, as light can reversibly modulate the monomer conformation that governs their mode of packing and resulting morphology.[15–18] However, most photoresponsive SP systems exhibit photocontrol over the degree of polymerization or drastic morphology changes by exploiting the different behaviors of the two photoisomers.[19–21] In contrast, inducing light-driven reorganization of the packing mode—together with changes in their higher-ordered aggregation state—without complete disassembly remains highly challenging.[22–24] We envisioned that a photoswitch capable of modulating conformational flexibility, rather than undergoing a drastic geometric transformation, could provide a subtle yet effective means to achieve this level of structural control.

Diarylethenes (DAEs) offer precisely this capability: the open-ring isomer (DAE_o) is conformationally flexible, whereas the closed-ring isomer (DAE_c) is rigid and more π-conjugated.[25,26] These DAE properties were previously incorporated in SP systems, exhibiting distinct differences in the SP morphologies between the two isomers.[27–37] Yet, photo-controlling the higher-ordered SP aggregation by leveraging the capability of DAEs has not been explored. Here, we show that a side-chain-functionalized DAE monomer (**1**, Fig. 1a) enables fully reversible

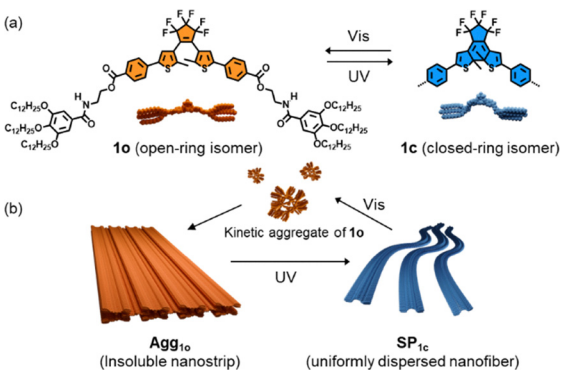

Fig. 1 (a) Molecular structures of **1** in the open-ring (**1o**) and closed-ring (**1c**) forms. (b) Schematic illustration of the photoswitchable self-assembly behavior of **1**, showing reversible interconversion between **1o** and **1c** under UV/Vis light irradiation and their respective assembly into $\mathbf{Agg_{1o}}$ (insoluble nanostrip) and $\mathbf{SP_{1c}}$ (soluble nanofiber).

[a] *Division of Advanced Science and Engineering, Graduate School of Science and Engineering, Chiba University, 1-33 Yayoi-cho, Inage-ku, Chiba 263-8522, Japan*
[b] *Department of Applied Physics, The University of Osaka, 2-1 Yamadaoka, Suita 565-0817, Japan*
[c] *Department of Creative Research, Exploratory Research Center on Life and Living Systems, National Institutes of Natural Sciences, Okazaki 444-8787, Japan*
[d] *Core Facility Center, Research Infrastructure Management Center, Institute of Science Tokyo, 4259 Nagatsuta, Midori-ku, Yokohama 226-8501, Japan*
[e] *Institute for Advanced Academic Research (IAAR), Chiba University, 1-33 Yayoi-cho, Inage-ku, Chiba 263-8522, Japan. E-mail: yagai@faculty.chiba-u.jp*
[f] *Department of Applied Chemistry and Biotechnology, Graduate School of Engineering, Chiba University, 1-33 Yayoi-cho, Inage-ku, Chiba 263-8522, Japan*

switching between a precipitated, ordered aggregate (nanostrip) and a uniformly dispersed supramolecular polymer (nanofiber) simply by alternating UV and visible light irradiation (Fig. 1b). To gain mechanistic insight, we directly visualize the photoinduced reorganization at the solid–liquid interface by high-speed atomic force microscopy (AFM), revealing anisotropic photoinduced dissolution of ordered aggregates followed by reassembly into uniformly dispersed supramolecular polymers.

Photoswitchable monomer **1** was synthesized according to Scheme S1 (supplementary information, SI) and characterized by ^{1}H and ^{13}C NMR spectroscopy and electrospray ionization mass spectrometry. ^{1}H NMR and UV/Vis absorption spectroscopy confirmed quantitative ring-opening to the open-ring isomer (**1o**) upon visible-light irradiation (λ = 620–645 nm). A hot solution of **1o** (c = 100 μM) in *n*-octane/$CHCl_3$ (95 : 5, v/v) was prepared by heating to 100 °C, followed by cooling to room temperature (r.t.), upon which the absorption band at 312 nm intensified and slightly blue-shifted to 310 nm (orange line in Fig. S1a, SI). Immediately after cooling, ill-defined aggregates were observed by AFM (Fig. S1b, SI). Upon aging the above solution of **1o** in the dark, the absorption intensity decreased while the band maximum red-shifted to 320 nm, accompanied by the formation of macroscopic precipitates (yellow line in Fig. S1a, SI). UV/Vis analysis of the supernatant after centrifugation showed that *ca.* 90% of the initially dissolved **1o** had been removed from solution as precipitates (Fig. S1d, SI). Increasing the initial concentration of **1o** accelerated the decrease in transmittance at 400 nm, indicating concentration-dependent precipitation behavior, consistent with precipitation from a supersaturated state generated upon cooling (Fig. S1c, SI). These results suggest that cooling initially produces metastable ill-defined aggregates, which subsequently undergo slow spectral change and macroscopic precipitation under the present conditions.[38–40]

Scanning electron microscopy (SEM) of the precipitates revealed an entangled fibrous microstructure (Fig. 2a and Fig. S2, SI). Hereafter, we refer to these precipitated aggregates of **1o** obtained by the cooling protocol as $\mathbf{Agg_{1o}}$. Powder X-ray diffraction (XRD) of $\mathbf{Agg_{1o}}$ displayed multiple reflections, most of which can be assigned to lamellar ordering with a *d*-spacing of 3.44 nm (Fig. 2b). Consistent with this, upon spin-coating a dispersion of $\mathbf{Agg_{1o}}$ onto a highly oriented pyrolytic graphite (HOPG) substrate, AFM imaging of the $\mathbf{Agg_{1o}}$ surface showed nanostrips with 8.31 nm periodicity and a thickness of 3.45 nm, observed as a single or multi-layer (Fig. 2c–e and Fig. S3, SI). Thus, despite its conformational flexibility, **1o** forms multi-layered nanostrips, which further associate to form macroscopic aggregates.

FT-IR spectroscopy of an $\mathbf{Agg_{1o}}$ film on a KBr plate showed an N–H vibrational band at 3238 cm^{-1} and a C=O stretching band at 1632 cm^{-1}, attributable to the amide groups. Compared with the monomeric state in $CHCl_3$ solution (ν_{N-H} = 3454 cm^{-1} and $\nu_{C=O}$ = 1659 cm^{-1}), both bands were markedly shifted to lower wavenumbers, indicating the formation of strong intermolecular hydrogen bonding in $\mathbf{Agg_{1o}}$ (Fig. S4a, SI). Upon UV-light irradiation (λ = 290 nm) of the $\mathbf{Agg_{1o}}$-coated KBr plate, the ring-closure

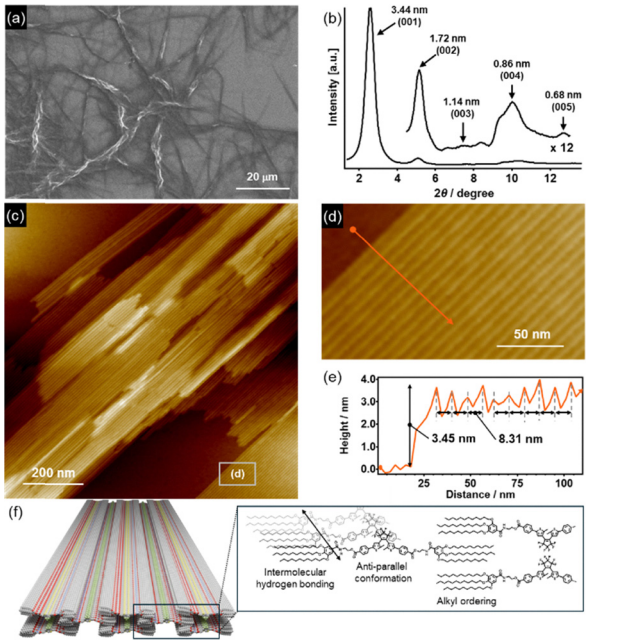

Fig. 2 (a) SEM image of the precipitated $\mathbf{Agg_{1o}}$. (b) Powder XRD pattern of the precipitated $\mathbf{Agg_{1o}}$ (c = 0.8 mM). (c) AFM image of $\mathbf{Agg_{1o}}$ and (d) a magnified view of the region in (c) enclosed by a white rectangle. (e) Cross-sectional analysis along an orange arrow in (d). (f) Proposed packing model of $\mathbf{Agg_{1o}}$.

reaction of the DAE_o moieties proceeded to give a ratio of **1o**/**1c** = 40 : 60 (determined by ^{1}H NMR), and the two bands shifted slightly to 3233 cm^{-1} and 1630 cm^{-1}, respectively. These results suggest that the DAE_o moieties in $\mathbf{Agg_{1o}}$ are preorganized in the photoreactive antiparallel conformation[41–43] and that ring closure to DAE_c occurs while largely preserving the hydrogen-bonding motif. Based on the above results and molecular modeling, we propose the packing model for $\mathbf{Agg_{1o}}$ shown in Fig. 2f. In this model, **1o** first forms a linear hydrogen-bonded chain through intermolecular N–H···O=C amide interactions. Along this chain, neighboring DAE_o units are further stabilized by π–π stacking interactions, which rigidify the assembly into a ribbon-like nanostrip. The methylene C–H stretching bands shifted slightly to lower wavenumbers upon aggregation (Fig. S4b, SI), indicating increased local conformational ordering of the alkyl chains.[44,45] The ordered supramolecular strands can further associate laterally, and the resulting two-dimensional sheets hierarchically stack, potentially assisted by short contacts involving C–F groups (*e.g.*, possible F···F close contacts), to form the layered structures. Because the present packing model cannot fully explain the observed 8.3 nm periodicity, further structural investigation, including attempts at single-crystal growth, is currently underway.

When a stirred dispersion of $\mathbf{Agg_{1o}}$ in *n*-octane/$CHCl_3$ (95 : 5, v/v) was irradiated at r.t. with UV light (λ = 290 nm, 3.4 mW cm^{-2}), a new broad absorption band centred at 593 nm grew, consistent with the ring-closure reaction to the DAE_c form (blue line in Fig. 3a). Concomitantly, the initial light scattering from the precipitate diminished, indicating photoinduced dissolution (Fig. 3b). The growth of the 592 nm band plateaued

after irradiation for 22 min, suggesting that the photostationary state under UV irradiation (PSS_{UV}) had been reached (Fig. S6a, SI). The **1o**/**1c** ratio at PSS_{UV} was 6 : 94 as determined by ^{1}H NMR, comparable to that measured in the monomeric state (Fig. S5, SI). AFM analysis of the resulting homogeneous solution, spin-coated onto an HOPG substrate, revealed flexible supramolecular polymers (**SP$_{1c}$**) with a width of 6.8 nm and a height of 1.2 nm (Fig. 3e–g). In contrast to **Agg$_{1o}$**, **SP$_{1c}$** remained dispersed for at least 14 days (Fig. S6a, SI).

To examine the self-assembly behavior of **1c** independent of the irradiation protocol, we studied its temperature-dependent aggregation. Upon heating the solution of **SP$_{1c}$** to 100 °C at a rate of 1.0 °C min^{-1}, the absorption bands around 400 nm and 600 nm shifted to shorter wavelengths, indicating weak interactions between DAE_c moieties (Fig. S6b, SI). Monitoring the absorbance at 415 nm revealed a non-sigmoidal dissociation curve, characteristic of a nucleation–elongation (cooperative) supramolecular polymerization mechanism.[46] Upon subsequent cooling, no thermal hysteresis was observed (Fig. S7a, SI). In accordance with this, AFM imaging of the cooled PSS_{UV} solution showed the same **SP$_{1c}$** morphology as that obtained by UV-light irradiation of **Agg$_{1o}$**, suggesting that, unlike **1o**, **1c** undergoes an equilibrium-controlled assembly process and the organization of **SP$_{1c}$** is independent of the self-assembly pathway (Fig. S7b–d, SI).

The morphology of **SP$_{1c}$** was further supported by *in situ* small-angle X-ray scattering (SAXS). The scattering profile was consistent with a long and cylindrical object and could be fitted with a core–shell cylinder model (r_{core} = 1.02 ± 0.01 nm, d_{shell} = 0.62 ± 0.1 nm, $l \geq 100$ nm) (Fig. 3c). The core radius nearly matches the size of the DAE_c moiety including the ester units on both sides (r = 0.96 nm) (Fig. S8, SI), supporting its face-to-face stacking arrangement (Fig. 3d). The smaller apparent outer diameter ($2(r_{core} + d_{shell}) \approx 3.3$ nm) compared with the AFM cross-section (6.8 nm) likely reflects the similarity of electron density at the alkyl spacers and in the solvent. FT-IR measurements of **SP$_{1c}$** in solution showed N–H and C=O stretching bands at 3295 and 1632 cm^{-1}, respectively (Fig. S6c, SI). Compared with **Agg$_{1o}$**, the N–H band exhibited a smaller shift from the monomeric state in $CHCl_3$, suggesting weaker hydrogen-bonding interactions in **SP$_{1c}$**. In the C–H stretching region, the FT-IR spectrum of **SP$_{1c}$** showed only minor differences from that of **Agg$_{1o}$**, suggesting that the local conformational ordering of the alkyl chains is comparable in the two assemblies (Fig. S6d, SI). We infer that the closed DAE_c unit, together with the protruding methyl group, introduces packing frustration between the face-to-face DAE_c stacking and the optimal geometry required for amide hydrogen bonding. Consequently, the monomers in **SP$_{1c}$** stack with reduced axial registry and weaker cooperative hydrogen bonding, leading to a lower degree of ordering along the supramolecular main chain and suppressing the development of distinct lateral organization.

The **Agg$_{1o}$** → **SP$_{1c}$** conversion under UV-light irradiation was directly observed using cell-equipped, tip-scan high-speed AFM (HS-AFM).[47] Because large aggregates hindered stable tip-scanning, **Agg$_{1o}$** was first fragmented by sonication (Fig. S9, SI). In the absence of UV light, the fragments remained stable at the solid–liquid interface between an HOPG substrate and *n*-octane and could be imaged continuously even under tapping forces (Fig. 3h and i, Movie S1). When UV light (λ = 365 nm, 4.8 mW cm^{-2}) was switched on after 60 s, we immediately

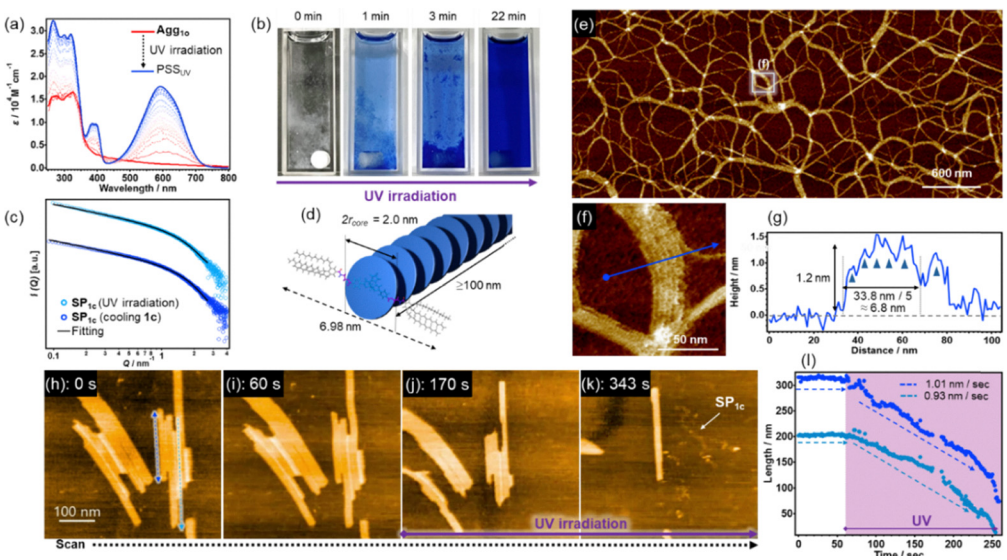

Fig. 3 (a) UV/vis absorption spectral changes of **1o** (c = 100 μM) in a 95 : 5 *n*-octane/$CHCl_3$ mixture before (red line) and after (blue line) UV-light irradiation (λ = 290 nm, 3.4 mW cm^{-2}) to reach a photostationary state (PSS_{UV}). (b) UV-induced dissolution process until reaching the PSS_{UV}. (c) SAXS profiles of **SP$_{1c}$** obtained either by UV-light irradiation to **Agg$_{1o}$** (pale blue) or by cooling **1c** (blue) (c = 300 μM). Black curves represent fitting with a "core–shell cylinder" model. (d) Schematic illustration of **SP$_{1c}$**. (e) AFM image of **SP$_{1c}$** and (f) a magnified image of bundled fibers in (e) enclosed by a white rectangle. (g) AFM cross-sectional analysis of bundled **SP$_{1c}$** along a blue arrow in (f). (h)–(k) Clipped HS-AFM images of fragmented **Agg$_{1o}$** upon UV-light irradiation (λ = 365 nm, 4.8 mW cm^{-2}) at the interface between a HOPG substrate and *n*-octane (see Video S1). (l) Length-change plots of **Agg$_{1o}$** along blue and pale blue double-headed arrows in (h) before and after UV-light irradiation.

observed anisotropic dissolution from the strip termini along the long axis at a rate of 1.0 nm s^{-1} (Fig. 3h–j, Movie S1 and Movie S2–S5). The dissolution proceeded linearly with time and was independent of the initial strip length (Fig. 3l), suggesting that the ring-closure reaction of DAE_o moieties at the exposed cross-section is the rate-determining step of the nanostrip dissolution.

Notably, dissolution always initiated from the termini rather than from within the nanostrip interior. Upon continued UV-light irradiation, the formation of $\mathbf{SP_{1c}}$ could be observed independently on the substrate (Fig. 3k and Movie S1). The continuous release of **1c** from the dissolving termini would increase its local concentration near the interface, potentially reaching the critical concentration required for $\mathbf{SP_{1c}}$ nucleation. The critical total concentration for $\mathbf{SP_{1c}}$ formation in bulk solution was estimated to be much lower than $c \approx 0.39$ μM in a solution experiment (Fig. S10, SI). Although interfacial conditions may differ from those in the bulk solution, the low critical concentration suggests that nucleation of **1c** can be readily induced upon its release. We could also image $\mathbf{SP_{1c}}$ directly by HS-AFM when a solution of $\mathbf{SP_{1c}}$ was deposited on an HOPG substrate (Movie S6). Together, these observations indicate that the $\mathbf{Agg_{1o}} \rightarrow \mathbf{SP_{1c}}$ conversion proceeds *via* an off-pathway route that involves dissolution into monomers (or small oligomeric species), followed by reassembly into $\mathbf{SP_{1c}}$.

Visible-light-induced ring opening of the DAE_c moieties in $\mathbf{SP_{1c}}$ regenerated $\mathbf{Agg_{1o}}$. When a solution of $\mathbf{SP_{1c}}$ was irradiated with visible light (620–645 nm, 69 mW cm^{-2}), the DAE_c absorption bands bleached quantitatively within 11 min (Fig. S11a, SI). Similar to the cooling protocol for **1o**, the solution transiently entered a supersaturated state containing ill-defined aggregates and subsequently yielded precipitates within a day (Fig. S12, SI). AFM and FT-IR measurements of the resulting precipitates confirmed the re-formation of $\mathbf{Agg_{1o}}$ (Fig. S11b, SI).

In conclusion, we have shown that aggregation of one-dimensional DAE supramolecular assemblies can be reversibly controlled by light through the interplay between the conformational flexibility of the DAE core and amide hydrogen bonding. The flexible ring-open isomer forms densely packed aggregates that promote macroscopic precipitation and insolubility, whereas the rigid ring-closed isomer assembles into soluble flexible nanofibers, thereby suppressing lateral organization. We anticipate that exploiting the switchable conformational freedom of DAEs will further expand the design space of reconfigurable supramolecular soft materials.

S. Y., K. M. and T. S. designed the project. K. M. and H. M. performed all the experimental work. K. M. and S. Y. prepared the overall manuscript, including figures. All authors, including T. U., C. G., T. K., S. D. and H. H., contributed by revising and/or commenting on the manuscript. S. Y. supervised the overall research.

Conflicts of interest

There are no conflicts to declare.

Data availability

The data that support the findings of this work have been included in the main text and supplementary information (SI). Supplementary information is available. See DOI: https://doi.org/10.1039/d6cc01370h.

Acknowledgements

This work was supported by the Japan Society for the Promotion of Science (JSPS) KAKENHI grant no. JP23H04873, JP23H04873 and JP24H01717, JP26H02288 through a Grant-in-Aid for Transformative Research Areas ''Materials Science of Meso-Hierarchy''. This work was performed under the approval of the Photon Factory Program Advisory Committee (Proposal No. 2024G542). The authors are grateful to Dr Hideaki Takagi and Dr Rie Haruki for the SAXS measurements.

References

1 T. Shimada, Y. Watanabe, T. Kajitani, M. Takeuchi, Y. Wakayama and K. Sugiyasu, *Chem. Sci.*, 2023, **14**, 822–826.
2 C. M. Atienza and L. Sánchez, *Chem. – Eur. J.*, 2024, **30**, e202400379.
3 S. Datta, Y. Yamada, R. Kudo and S. Yagai, *Macromolecules*, 2026, **59**, 1069–1084.
4 L. López-Gandul, G. Lavarda, B. W. L. Van Den Bersselaar, G. Vantomme, E. W. Meijer and L. Sánchez, *Chem. Sci.*, 2024, **15**, 14037–14043.
5 N. Bäumer, E. Castellanos, B. Soberats and G. Fernández, *Nat. Commun.*, 2023, **14**, 1084.
6 S. Sarkar, A. Sarkar, A. Som, S. S. Agasti and S. J. George, *J. Am. Chem. Soc.*, 2021, **143**, 11777–11787.
7 R. Laishram, S. Sarkar, I. Seth, N. Khatun, V. K. Aswal, U. Maitra and S. J. George, *J. Am. Chem. Soc.*, 2022, **144**, 11306–11315.
8 P. Khanra, P. Rajdev and A. Das, *Angew. Chem., Int. Ed.*, 2024, **63**, e202400486.
9 M. Wehner, M. I. S. Röhr, M. Bühler, V. Stepanenko, W. Wagner and F. Würthner, *J. Am. Chem. Soc.*, 2019, **141**, 6092–6107.
10 C. Otsuka, S. Takahashi, A. Isobe, T. Saito, T. Aizawa, R. Tsuchida, S. Yamashita, K. Harano, H. Hanayama, N. Shimizu, H. Takagi, R. Haruki, L. Liu, M. J. Hollamby, T. Ohkubo and S. Yagai, *J. Am. Chem. Soc.*, 2023, **145**, 22563–22576.
11 C. Otsuka, S. Imai, T. Ohkubo and S. Yagai, *Chem. Commun.*, 2024, **60**, 1108–1111.
12 Y. Kasahara, T. Takeda, S. Dekura, Y. Ishii, H. Anetai, A. Takai, I. Hisaki, M. Takeuchi and T. Akutagawa, *J. Am. Chem. Soc.*, 2025, **147**, 18783–18795.
13 C. Montañez-Moyano, Y. Xue, M. V. Cappellari, A. Martínez-Manjarrés, L. Borsdorf, C. A. Strassert and G. Fernández, *Angew. Chem., Int. Ed.*, 2025, **64**, e202509031.
14 S. Datta and D. Chaudhuri, *Angew. Chem., Int. Ed.*, 2022, **61**, e202201956.
15 S. Yagai and A. Kitamura, *Chem. Soc. Rev.*, 2008, **37**, 1520.
16 F. Xu and B. L. Feringa, *Adv. Mater.*, 2023, **35**, 2204413.
17 S. Yagai, T. Iwashima, K. Kishikawa, S. Nakahara, T. Karatsu and A. Kitamura, *Chem. – Eur. J.*, 2006, **12**, 3984–3994.
18 E. Weyandt, G. M. Ter Huurne, G. Vantomme, A. J. Markvoort, A. R. A. Palmans and E. W. Meijer, *J. Am. Chem. Soc.*, 2020, **142**, 6295–6303.
19 M. Endo, T. Fukui, S. H. Jung, S. Yagai, M. Takeuchi and K. Sugiyasu, *J. Am. Chem. Soc.*, 2016, **138**, 14347–14353.
20 F. Xu, L. Pfeifer, S. Crespi, F. K.-C. Leung, M. C. A. Stuart, S. J. Wezenberg and B. L. Feringa, *J. Am. Chem. Soc.*, 2021, **143**, 5990–5997.
21 L.-H. Cheung, T. Kajitani and F. K.-C. Leung, *J. Colloid Interface Sci.*, 2022, **628**, 984–993.
22 T. Fukushima, K. Tamaki, A. Isobe, T. Hirose, N. Shimizu, H. Takagi, R. Haruki, S. Adachi, M. J. Hollamby and S. Yagai, *J. Am. Chem. Soc.*, 2021, **143**, 5845–5854.

23 T. Muraoka, H. Cui and S. I. Stupp, *J. Am. Chem. Soc.*, 2008, **130**, 2946–2947.
24 L. Li, H. Jiang, B. W. Messmore, S. R. Bull and S. I. Stupp, *Angew. Chem., Int. Ed.*, 2007, **46**, 5873–5876.
25 M. Irie, *Chem. Rev.*, 2000, **100**, 1685–1716.
26 M. Irie, T. Fukaminato, K. Matsuda and S. Kobatake, *Chem. Rev.*, 2014, **114**, 12174–12277.
27 T. Hirose and K. Matsuda, *Org. Biomol. Chem.*, 2013, **11**, 873.
28 K. Higashiguchi, G. Taira, J. Kitai, T. Hirose and K. Matsuda, *J. Am. Chem. Soc.*, 2015, **137**, 2722–2729.
29 S. Yagai, K. Iwai, M. Yamauchi, T. Karatsu, A. Kitamura, S. Uemura, M. Morimoto, H. Wang and F. Würthner, *Angew. Chem., Int. Ed.*, 2014, **53**, 2602–2606.
30 S. Yagai, K. Ishiwatari, X. Lin, T. Karatsu, A. Kitamura and S. Uemura, *Chem. – Eur. J.*, 2013, **19**, 6971–6975.
31 Y. Cai, Z. Guo, J. Chen, W. Li, L. Zhong, Y. Gao, L. Jiang, L. Chi, H. Tian and W.-H. Zhu, *J. Am. Chem. Soc.*, 2016, **138**, 2219–2224.
32 D. J. van Dijken, J. M. Beierle, M. C. A. Stuart, W. Szymański, W. R. Browne and B. L. Feringa, *Angew. Chem., Int. Ed.*, 2014, **53**, 5073–5077.
33 J. J. D. De Jong, L. N. Lucas, R. M. Kellogg, J. H. Van Esch and B. L. Feringa, *Science*, 2004, **304**, 278–281.
34 L. N. Lucas, J. Van Esch, B. L. Feringa and R. M. Kellogg, *Chem. Commun.*, 2001, 759–760.
35 S. Yokoyama, T. Hirose and K. Matsuda, *Chem. Commun.*, 2014, **50**, 5964–5966.
36 S. Li, T. Xiao, W. Xia, X. Ding, Y. Yu, J. Jiang and L. Wang, *Chem. – Eur. J.*, 2011, **17**, 10716–10723.
37 S. Yagai, K. Ohta, M. Gushiken, K. Iwai, A. Asano, S. Seki, Y. Kikkawa, M. Morimoto, A. Kitamura and T. Karatsu, *Chem. – Eur. J.*, 2012, **18**, 2244–2253.
38 P. A. Korevaar, S. J. George, A. J. Markvoort, M. M. J. Smulders, P. A. J. Hilbers, A. P. H. J. Schenning, T. F. A. De Greef and E. W. Meijer, *Nature*, 2012, **481**, 492–496.
39 A. J. Dear, G. Meisl, A. Šarić, T. C. T. Michaels, M. Kjaergaard, S. Linse and T. P. J. Knowles, *Chem. Sci.*, 2020, **11**, 6236–6247.
40 M. Wehner, M. I. S. Röhr, M. Bühler, V. Stepanenko, W. Wagner and F. Würthner, *J. Am. Chem. Soc.*, 2019, **141**, 6092–6107.
41 C. Bertarelli, M. C. Gallazzi, F. Stellacci, G. Zerbi, S. Stagira, M. Nisoli and S. De Silvestri, *Chem. Phys. Lett.*, 2002, **359**, 278–282.
42 S. Kobatake, K. Uchida, E. Tsuchida and M. Irie, *Chem. Commun.*, 2002, 2804–2805.
43 M. Morimoto, S. Kobatake and M. Irie, *Chem. – Eur. J.*, 2003, **9**, 621–627.
44 K. Tamaki, H. Hanayama, S. Datta, F. Silly, Y. Wada, D. Hashizume, K. Adachi, T. Uchihashi, M. Kawano, C. Ganser and S. Yagai, *Chem*, 2026, **12**, 102818.
45 C. Zhang, H. Pan and Y. Zhou, *Macromolecules*, 2023, **56**, 7870–7878.
46 M. M. J. Smulders, M. M. L. Nieuwenhuizen, T. F. A. de Greef, P. van der Schoot, A. P. H. J. Schenning and E. W. Meijer, *Chem. – Eur. J.*, 2010, **16**, 362–367.
47 H. Matsui, C. Ganser, K. Tamaki, Q. Liu, F.-Y. Chan, T. Uchihashi, P. Verma, Y. Sagara, S. Yagai and T. Umakoshi, *Langmuir*, 2026, **42**, 448–454.

